ROYAL SOCIETY OPEN SCIENCE

Research

Check for updates

Author for correspondence:
Jo Shien Ng
e-mail: j.s.ng@sheffield.ac.uk

†Present address: School of Physics and Astronomy, Cardiff University, Cardiff CF24 3AA, UK.

THE ROYAL SOCIETY PUBLISHING

Thin $Al_{1-x}Ga_xAs_{0.56}Sb_{0.44}$ diodes with extremely weak temperature dependence of avalanche breakdown

Xinxin Zhou, Chee Hing Tan, Shiyong Zhang, Manuel Moreno, Shiyu Xie†, Salman Abdullah and Jo Shien Ng

Department of Electronic and Electrical Engineering, University of Sheffield, Sheffield S1 3JD, UK

JSN, 0000-0002-1064-0410

When using avalanche photodiodes (APDs) in applications, temperature dependence of avalanche breakdown voltage is one of the performance parameters to be considered. Hence, novel materials developed for APDs require dedicated experimental studies. We have carried out such a study on thin $Al_{1-x}Ga_xAs_{0.56}Sb_{0.44}$ p–i–n diode wafers (Ga composition from 0 to 0.15), plus measurements of avalanche gain and dark current. Based on data obtained from 77 to 297 K, the alloys $Al_{1-x}Ga_xAs_{0.56}Sb_{0.44}$ exhibited weak temperature dependence of avalanche gain and breakdown voltage, with temperature coefficient approximately $0.86–1.08\,mV\,K^{-1}$, among the lowest values reported for a number of semiconductor materials. Considering no significant tunnelling current was observed at room temperature at typical operating conditions, the alloys $Al_{1-x}Ga_xAs_{0.56}Sb_{0.44}$ (Ga from 0 to 0.15) are suitable for InP substrates-based APDs that require excellent temperature stability without high tunnelling current.

1. Introduction

Avalanche photodiodes (APDs) are widely used in optical communication, imaging and sensing applications that require detection of high speed and/or weak optical signals. When the noise is dominated by the amplifier, the APD improves the system signal to noise ratio, by amplifying the photo-generated current through the impact ionization process. A cascade of impact ionization events can transform a single electron (or hole) into an avalanche of new carriers, leading to a large external current. In most semiconductor materials, the ionization process is stochastic and hence a mean avalanche gain, M, is measured in practice.

Avalanche gain versus reverse bias characteristic, $M(V)$, of an APD can be highly temperature-sensitive; therefore, a control

circuit is essential for accurately adjusting the reverse bias (or the operating temperature) to maintain M. When the APD is operated in the Geiger mode, the temperature dependence of avalanche gain can lead to significant changes in the breakdown probability, which in turn governs the photon detection probability and the dark counts. Hence, APDs with temperature-insensitive $M(V)$ characteristics that require minimal temperature stabilization control are highly desirable.

Temperature sensitivity of an APD is characterized by the temperature coefficient of its avalanche breakdown voltage, $C_{bd} = \Delta V_{bd}/\Delta T$, where ΔV_{bd} and ΔT are changes in breakdown voltage and temperature, respectively. For a given avalanche material, C_{bd} increases with avalanche region width, w [1,2]. This is illustrated by C_{bd} values of 6 and $11\,\text{mV}\,\text{K}^{-1}$ reported for InP diodes with $w = 130$ and 250 nm, respectively [1]. Although reducing w leads to reduced C_{bd}, there exists a lower limit for w, imposed by the band- to-band tunnelling current from the avalanche region, which is subjected to high electric field. For example, for APDs used in $10\,\text{Gbit}\,\text{s}^{-1}$ optical communication receivers, the approximate lower limits for avalanche materials InP and InAlAs are $w = 180$ and 150 nm, respectively [3].

The material $AlAs_{0.56}Sb_{0.44}$ (AlAsSb), which is lattice matched to InP substrates, has been investigated as avalanche material for APDs grown on InP substrates [4]. In [4], an AlAsSb diode with $w = 80\,\text{nm}$ exhibited the smallest C_{bd} value ($0.95\,\text{mV}\,\text{K}^{-1}$) reported in the literature for comparable w (where the breakdown mechanism is dominated by avalanche breakdown in all data compared). Besides the low C_{bd} value, AlAsSb also exhibit very low excess noise factor ($F = 2.15$ at $M = 10$) [5], comparable to that of silicon APD. While exhibiting low excess noise and C_{bd} value, the high Al composition is vulnerable to oxidization, which gives higher leakage currents [6]. Incorporating Gallium into AlAsSb was reported to significantly reduce the oxidation rate [7]. More recently, alloys of $Al_{1-x}Ga_xAs_{0.56}Sb_{0.44}$ ($x = 0$, 0.05, 0.1, 0.15), also lattice-matched to InP substrates, were found to have substantially lower room temperature surface leakage current for alloys with $x = 0.1$ and 0.15 [6]. From $AlAs_{0.56}Sb_{0.44}$ to $Al_{0.85}Ga_{0.15}As_{0.56}Sb_{0.44}$, the bandgap reduces very slightly from 1.64 to 1.56 eV [6]. Crucially, the reduced bandgap did not lead to significant band-to-band tunnelling current, suggesting that $Al_{1-x}Ga_xAs_{0.56}Sb_{0.44}$ could be an attractive material for low tunnelling, low surface leakage avalanche region. Thus, a thin $Al_{0.85}Ga_{0.15}As_{0.56}Sb_{0.44}$ avalanche layer was used to achieve an APD with very high gain–bandwidth product of 424 GHz [8]. For a more comprehensive assessment of $Al_{1-x}Ga_xAs_{0.56}Sb_{0.44}$ alloys, lattice matched to InP, it is important to consider their temperature sensitivity of dark current and avalanche breakdown, which has not been reported. Note that these alloys have larger bandgap than, and distinct band structures from, the $Al_{1-x}Ga_xAs_{1-y}Sb_y$ alloys ($x = 0.40$–0.65 and $y = 0.035$–0.054) grown lattice-matched to GaSb substrates [9].

In this work, we report the temperature dependence of $M(V)$, from which the C_{bd} values for $Al_{1-x}Ga_xAs_{0.56}Sb_{0.44}$ p^+in^+ diodes, with $x = 0$, 0.05, 0.1 and 0.15, were obtained. The diodes have nominal $w = 100\,\text{nm}$, a useful value for designing high-speed APDs. Levels of dark currents from $Al_{1-x}Ga_xAs_{0.56}Sb_{0.44}$ were also compared with those from InP and InAlAs, current avalanche materials in APDs latticed-matched to InP substrates.

2. Experimental details

The $Al_{1-x}Ga_xAs_{0.56}Sb_{0.44}$ ($Al_{1-x}Ga_xAsSb$) p^+in^+ diode wafers with $x = 0$, 0.05, 0.1, 0.15 used in this work are identical to those described in [6]. The wafers were grown by molecular beam epitaxy on InP substrate using Be and Si as p-type and n-type dopants, respectively. Structure details of the wafers are shown schematically in figure 1a. The wafers were fabricated into circular mesa diodes with nominal diameters, D of 400, 200, 100 and 50 μm using standard photolithography and wet chemical etch. The p- and n-metal contacts were formed by Ti–Au.

Capacitance–voltage (C–V) measurements on each wafer were performed at room temperature. Fittings to the C–V characteristics then gave estimated values of w as well as the approximate doping concentrations in the claddings and the i-region [6]. Secondary ion mass spectroscopy data (p- and n-type dopant atoms profiles) from the $x = 0.15$ wafer, as shown in figure 1b, support the information obtained from C–V characteristics. The deduced w values range from 110 to 116 nm, slightly thicker than the nominal 100 nm, as summarized in table 1.

Avalanche gain measurements were carried out at temperatures of 77, 150, 200, 250 and 297 K, using a Janis ST-500 low-temperature probe station. The measurements relied on phase-sensitive detection of photocurrent versus reverse bias, $I_{ph}(V)$, so that the photocurrent data were unaffected by background radiation, background noise and diode's dark current. A 542 nm wavelength He–Ne laser
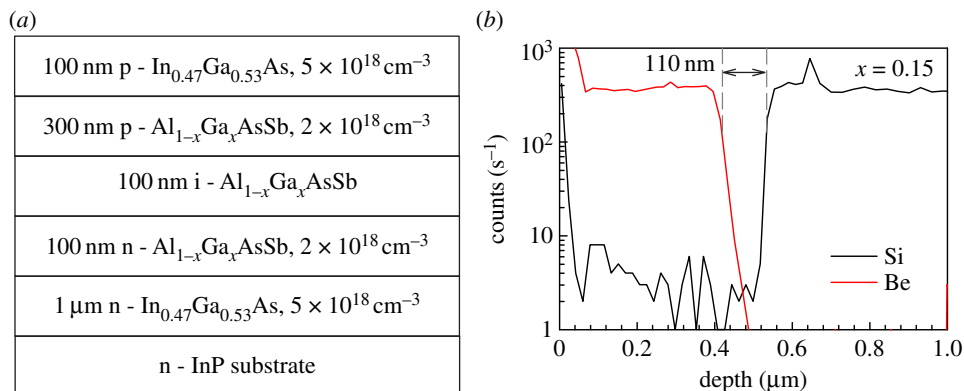
Figure 1. (a) Structure details of $Al_{1-x}Ga_xAs_{0.56}Sb_{0.44}$ wafers and (b) secondary-ion-mass spectroscopy data of the $Al_{0.85}Ga_{0.15}AsSb$ diode.

Table 1. Avalanche region width, bandgap and deduced C_{bd} of the wafers.

material	w (nm) [6]	E_g (eV) [6]	C_{bd} (mV/K)
$AlAs_{0.56}Sb_{0.44}$	111	1.64	1.07–1.08
$Al_{0.95}Ga_{0.05}As_{0.56}Sb_{0.44}$	116	1.61	1.03–1.05
$Al_{0.9}Ga_{0.1}As_{0.56}Sb_{0.44}$	114	1.59	0.95–0.96
$Al_{0.85}Ga_{0.15}As_{0.56}Sb_{0.44}$	110	1.56	0.86–0.91

light, mechanically chopped at 170 Hz, was used to produce the photocurrent (measured with lock-in amplifier). Dividing $I_{ph}(V)$ with the injected primary photocurrent at low bias gave $M(V)$. The V_{bd} for a given device was then obtained from the horizontal intercept of its $1/M$ versus V plot. For a given wafer and temperature, $M(V)$ were measured from two devices.

To assess uniformity of V_{bd} value across a given wafer and to support the V_{bd} value derived from $M(V)$, characteristics of reverse dark current versus reverse bias voltage, $I–V$, was measured from seven devices (three of $D = 400\,\mu m$, two of $D = 200\,\mu m$ and two of $D = 100\,\mu m$) from each of the wafers at the same temperature points. These measurements were performed using the low-temperature probe station too, and they confirmed that the breakdown voltage is consistent across a given wafer.

3. Results

The data of $M(V)$ for all four wafers from 77 to 297 K are shown in figure 2. Results shown were obtained from diodes with $D = 400\,\mu m$. For each alloy, at a given reverse bias, decreasing the temperature increases M, which is the typical temperature dependence for avalanche multiplication in most wide bandgap semiconductor materials. Data of $1/M$ versus V and linear fittings to extract V_{bd} values from one of the devices on all four alloys are shown in figure 3.

The deduced V_{bd} values are plotted against temperature for all the alloys in figure 4. The data can be described with linear fittings (with gradients of C_{bd}) over the range of temperature studied. The values of C_{bd} ranging from 0.86 to 1.08 mV K^{-1} are listed in table 1. The C_{bd} values for all four alloys are similar, within accuracy of our experimental set-up.

The breakdown voltage values deduced using extrapolation of $1/M$ from two devices for each alloy are shown in figure 4. These values are supported by the breakdown voltage obtained from the reverse $I–V$ data. For a given wafer, the seven sets of reverse $I–V$ data exhibited abrupt breakdown at highly similar voltages, indicating highly uniform diodes. The typical reverse $I–V$ data of the $D = 400\,\mu m$ diodes at different temperatures are plotted in figure 5 for the four alloys. For each alloy, an abrupt breakdown in dark current can be observed at all temperatures, for reverse bias voltage near the V_{bd} deduced from avalanche gain measurements (indicated in figure 5).

Observing figure 5, higher dark currents are present in wafers with higher Al content (smaller x). For a given diode, current densities (current divided by device area, not shown here) from different-sized
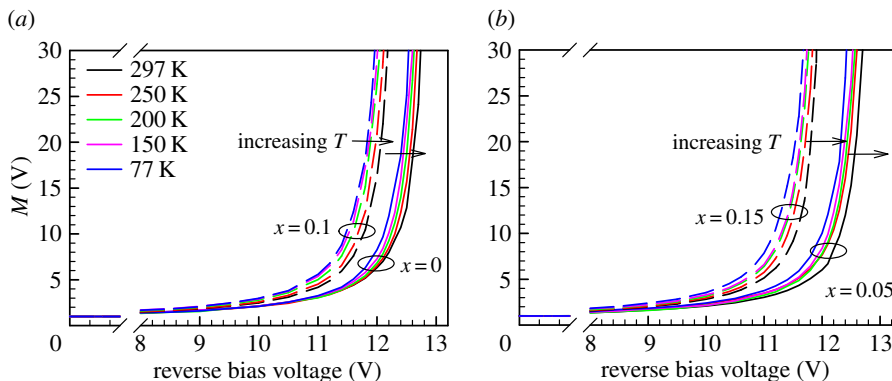
Figure 2. Avalanche gain characteristics from 77 to 297 K of the $Al_{1−x}Ga_xAsSb$ diodes with (*a*) $x = 0$ and 0.10 and (*b*) $x = 0.05$ and 0.15.
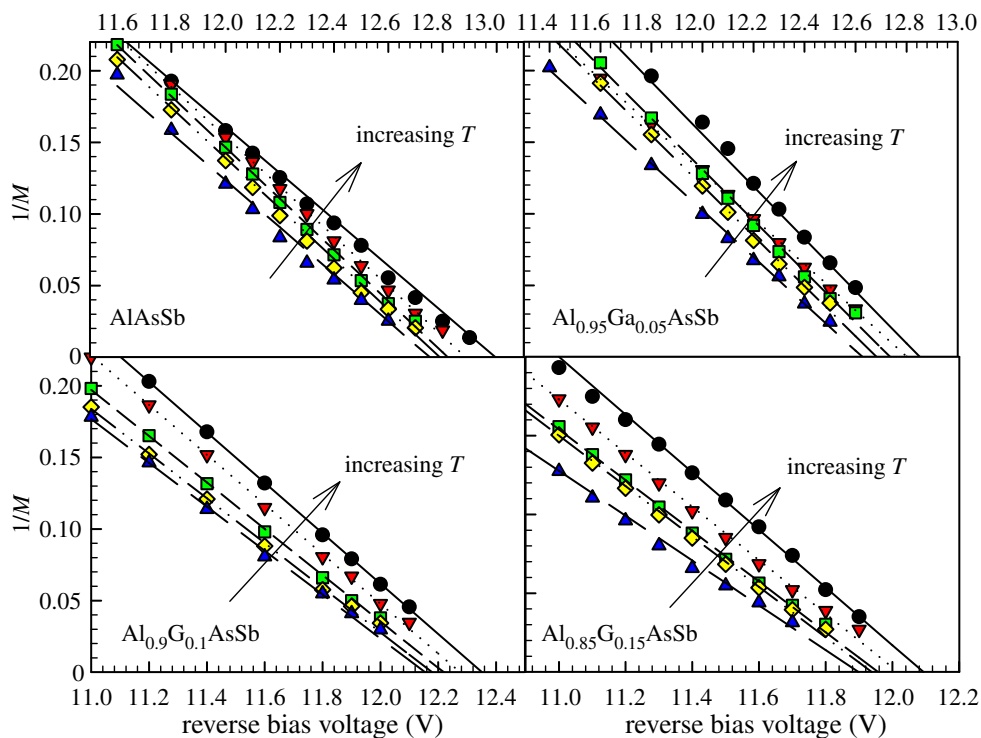
Figure 3. Data of $1/M$ versus reverse bias (symbols) and linear fittings (lines) of the $Al_{1−x}Ga_xAsSb$ diodes at 77, 150, 200, 250 and 297 K.
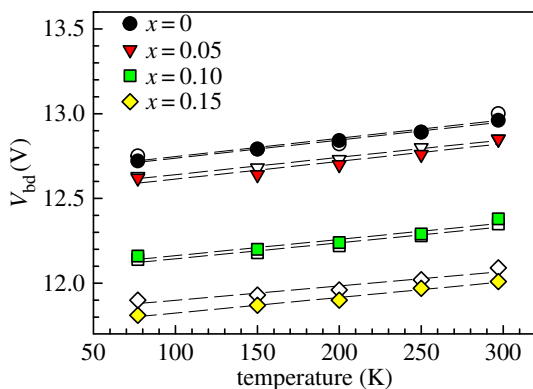
Figure 4. Experimental breakdown voltage versus temperature (symbols) and linear fittings (lines) for the $Al_{1−x}Ga_xAs_{0.56}Sb_{0.44}$ diode wafers ($x = 0$–0.15). Two sets of data were obtained for each wafer.
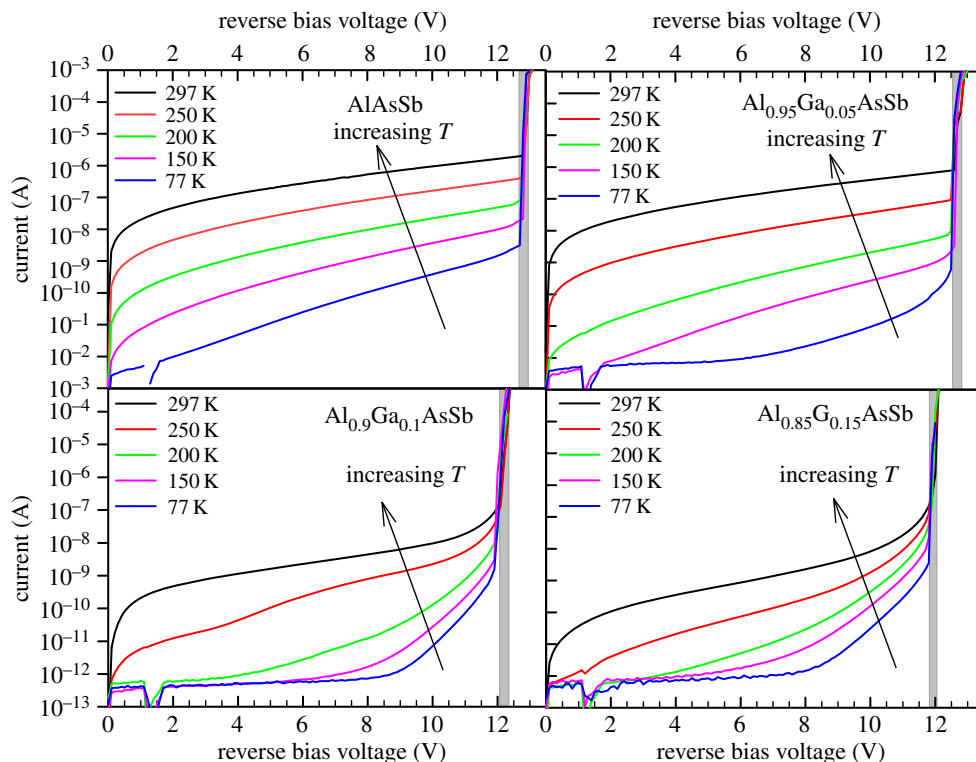
Figure 5. Dark current characteristics (colour lines) and V_{bd} deduced from $M(V)$ data (shaded regions) at 77–297 K of the $Al_{1-x}Ga_xAsSb$ diodes.

devices at low reverse bias (0 to approx. 8.5 V) showed disagreement, indicating that those dark currents are mainly from surface leakage mechanisms. As temperature falls, these surface leakage currents decrease rapidly, until the measurements of dark current became limited by the measurement system (approx. 0.5 pA).

4. Discussion

In figure 6a, the temperature coefficients of breakdown voltage of this work are compared with relevant reports from the literature. Considering only the $AlAs_{0.56}Sb_{0.44}$ data from this work and reference [4], C_{bd} increases with w, as observed on other semiconductors.

The data from this work are also compared with semiconductors used in the avalanche region of InP-based APDs (InP and InAlAs) in figure 6a. For a given w, the $Al_{1-x}Ga_xAsSb$ diodes have very small C_{bd}, in line with the C_{bd} of $AlAs_{0.56}Sb_{0.44}$ diodes from Xie & Tan [4] and much lower than those of InP and InAlAs diodes.

Alloy disorder potential analyses in [11] indicated that the very small C_{bd} values for $AlAs_{0.56}Sb_{0.44}$ diodes could have originated from significant alloy scattering, because of very different covalent radii of the Sb and As atoms. The ratio between the As and the Sb is the same for the $AlAs_{0.56}Sb_{0.44}$ and the $Al_{1-x}Ga_xAs_{0.56}Sb_{0.44}$ diodes, hence similarly small C_{bd} are perhaps not surprising for the $Al_{1-x}Ga_xAs_{0.56}Sb_{0.44}$ diodes in this work.

The experimental $I-V$ characteristics from figure 5 facilitate a comparison of the reverse current density from $Al_{1-x}Ga_xAsSb$ with those from the current avalanche materials of choices, InP and InAlAs. In figure 6b, simulated band-to-band tunnelling current density versus electric field from InP [1] and InAlAs [10] p^+in^+ diodes with $w = 110$ nm are plotted, with conditions of $0.95\,V_{bd}$ indicated by symbols. Also plotted are the gain-normalized dark current densities at electric fields corresponding to $0.95\,V_{bd}$ from our diodes with $x = 0.10$ and 0.15. At conditions of $0.95\,V_{bd}$, the dark current densities in our diodes are approximately 5×10^{-6} A cm^{-2}, at least 5 and 3 orders of magnitude lower than those of InP and InAlAs, respectively. The simulated tunnelling current for thin InAlAs diode is consistent with the level from a waveguide InGaAs/InAlAs APD using an 100 nm thick InAlAs avalanche layer ($0.95\,V_{bd}$
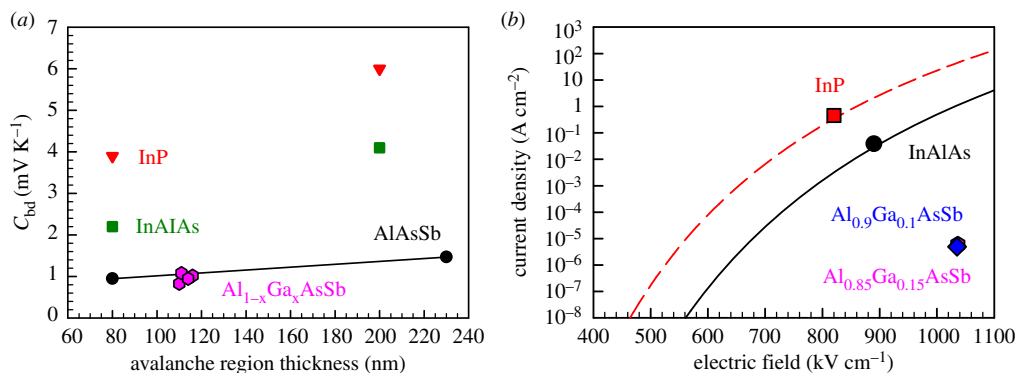
Figure 6. (a) Comparison of C_{bd} in AlGaAsSb of this work with those for InP, InAlAs [1] and AlAs$_{0.56}$Sb$_{0.44}$ [4]. (b) Room temperature comparison of simulated tunnelling current densities for InP [1] and InAlAs [10] diodes with $w = 110$ nm, as well as experimental unmultiplied dark current density of the Al$_{0.9}$Ga$_{0.1}$As$_{0.56}$Sb$_{0.44}$ and Al$_{0.85}$Ga$_{0.15}$As$_{0.56}$Sb$_{0.44}$ diodes at 0.95 V_{bd}.

of 0.096 A cm^{-2}) [12]. Our results confirm the potential of using thin AlGaAsSb as a low dark current avalanche region.

5. Conclusion

Four Al$_{1-x}$Ga$_x$As$_{0.56}$Sb$_{0.44}$ p–i–n diode wafers with 110–116 nm avalanche region width and Ga composition of $x = 0$, 0.05, 0.10 and 0.15 were characterized, in the experimental study on temperature dependence of breakdown voltage, avalanche gain and dark current. All four wafers showed weak temperature dependence of breakdown voltage and avalanche gain, with C_{bd} ranging from 0.86 to 1.08 mV K^{-1}, among the lowest values ever reported for a wide range of semiconductor materials. Combined with much lower dark current density (compared with tunnelling current densities in InP and InAlAs), the Al$_{1-x}$Ga$_x$As$_{0.56}$Sb$_{0.44}$ materials are promising as avalanche layers in InP substrates-based APDs that require excellent temperature insensitivity.

References

1. Tan LJJ, Ong DSG, Ng JS, Tan CH, Jones SK, Qian YH, David JPR. 2010 Temperature dependence of avalanche breakdown in InP and InAlAs. *IEEE J. Quantum Electron.* **46**, 1153–1157. (doi:10.1109/JQE.2010.2044370)

2. Massey DJ, David JPR, Rees GJ. 2006 Temperature dependence of impact ionization in submicrometer silicon devices. *IEEE Trans. Electron Devices* **53**, 2328–2334. (doi:10.1109/TED.2006.881010)

3. Ong DSG, Hayat MM, David JPR, Ng JS. 2011 Sensitivity of high-speed lightwave system receivers using InAlAs avalanche photodiodes. *IEEE Photon. Technol. Let.* **23**, 233–235. (doi:10.1109/LPT.2010.2098862)

4. Xie S, Tan CH. 2011 AlAsSb avalanche photodiodes with a sub-mV/K temperature coefficient of breakdown voltage. *IEEE J. Quantum Electron.* **47**, 1391–1395. (doi:10.1109/JQE.2011.2165051)

5. Xie J, Xie S, Tozer RC, Tan CH. 2012 Excess noise characteristics of thin AlAsSb APDs. *IEEE Trans. Electron. Devices* **59**, 1475–1479. (doi:10.1109/TED.2012.2187211)

6. Zhou X, Zhang S, David JPR, Ng JS, Tan CH. 2016 Avalanche breakdown characteristics of Al$_{1-x}$Ga$_x$As$_{0.56}$Sb$_{0.44}$ quaternary alloys. *IEEE Photon. Technol. Let.* **28**, 2495–2498. (doi:10.1109/LPT.2016.2601651)

7. Mathis SK, Lau KHA, Andrews AM, Hall EM, Almuneau G, Hu EL, Speck JS. 2001 Lateral oxidation kinetics of AlAsSb and related alloys lattice matched to InP. *J. Appl. Phys.* **89**, 2458–2464. (doi:10.1063/1.1335825)

8. Xie S, Zhou X, Zhang S, Thomson DJ, Chen X, Reed GT, Ng JS, Tan CH. 2016 InGaAs/AlGaAsSb avalanche photodiode with high gain-bandwidth product. *Opt. Express* **24**, 24 242–24 247. (doi:10.1364/OE.24.024242)

9. Grzesik M, Donnelly J, Duerr E, Manfra M, Diagne M, Bailey R, Turner G, Goodhue W. 2014 Impact ionization in Al$_x$Ga$_{1-x}$As$_y$Sb$_{1-y}$ avalanche photodiodes. *Appl. Phys. Lett.* **104**, 162103. (doi:10.1063/1.4872253)

10. Goh YL *et al.* 2007 Avalanche multiplication in InAlAs. *IEEE Trans. Electron Devices* **54**, 11–16. (doi:10.1109/TED.2006. 887229)

11. Ong JSL, Ng JS, Krysa AB, David JPR. 2014 Temperature dependence of avalanche multiplication and breakdown voltage in $Al_{0.52}In_{0.48}P$. *J. Appl. Phys.* **115**, 064 507–064 512. (doi:10.1063/1.4865743)

12. Makita K, Nakata T, Shiba K, Kakeuchi T. 2005 40Gbps waveguide photodiode. *J. Adv. Tech.* **2**, 234–240.

13. Zhou X, Tan CH, Zhang S, Moreno M, Xie S, Abdullah S, Ng JS. 2017 Data from: Thin $Al1-xGaxAs0.56Sb0.44$ diodes with extremely weak temperature dependence of avalanche breakdown. Data Dryad Repository. (http://dx.doi. org/10.5061/dryad.2f1k2)